Novel Search for Heavy ν Mixing from the β^+ Decay of ^{38m}K Confined in an Atom Trap

M. Trinczek,[1,*] A. Gorelov,[1] D. Melconian,[1] W. P. Alford,[2] D. Asgeirsson,[3] D. Ashery,[4] J. A. Behr,[3] P. G. Bricault,[3] J. M. D'Auria,[1] J. Deutsch,[5] J. Dilling,[6,3] M. Dombsky,[3] P. Dubé,[1] S. Eaton,[3] J. Fingler,[3] U. Giesen,[3] S. Gu,[3] O. Häusser,[1,†] K. P. Jackson,[3] B. Lee,[3] J. H. Schmid,[6] T. J. Stocki,[1] T. B. Swanson,[1] and W. Wong[3]

[1]*Simon Fraser University, Burnaby, British Columbia, Canada V5A 1S6*
[2]*University of Western Ontario, London, Ontario, Canada N6A 3K7*
[3]*TRIUMF, 4004 Wesbrook Mall, Vancouver, British Columbia, Canada V6T 2A3*
[4]*Tel Aviv University, 69978 Tel Aviv, Israel*
[5]*Université Catholique de Louvain, B-1348 Louvain-la-Neuve, Belgium*
[6]*Physikalisches Institut der Universität Heidelberg, 69120 Heidelberg, Germany*

(Received 19 March 2002; published 2 January 2003)

A new technique, full neutrino momentum reconstruction, is used to set limits on the admixture of heavy neutrinos into the electron neutrino. We measure coincidences between nuclear recoils and positrons from the beta decay of trapped radioactive atoms and deduce the neutrino momentum. A search for peaks in the reconstructed recoil time-of-flight spectrum as a function of positron energy is performed. The admixture upper limits range from 4×10^{-3} to 2×10^{-2} and are the best direct limits for neutrinos (as opposed to antineutrinos) for the mass region of 0.7 to 3.5 MeV.

DOI: 10.1103/PhysRevLett.90.012501 PACS numbers: 23.40.Bw, 14.60.Pq, 32.80.Pj

There is now good evidence from solar [1] and atmospheric [2] neutrino oscillation experiments for finite neutrino masses with two values of Δm^2, both $<10^{-2}$ eV^2. However, small admixtures of very heavy neutrinos into the electron neutrino remain possible. Although sterile neutrino admixtures are excluded with high confidence as explanations of atmospheric and solar neutrino mixing, the small admixture/heavy neutrino range explored by this paper remains open. Constraints from supernova SN1987A also allow ν_e to have relatively large admixtures with a sterile neutrino whose mass is a few MeV [3].

Traditional searches for massive neutrino admixtures in nuclear β decay look for subtle kinks in continuous β energy spectra [4]. We employ a new technique: full neutrino momentum reconstruction. Since nuclear β decay is a three-body process, and we observe the positron and the recoiling daughter nucleus in coincidence, the missing neutrino momentum can be deduced. A magneto-optical trap (MOT) [5] holds the atoms suspended in space by laser light and a weak magnetic quadrupole field. A unique advantage of our technique is the ability to observe the momenta of the recoiling daughter atom and the positron free of distortions as both easily escape the shallow trap potential. Using the relativistic β as a trigger, we accurately measure the time of flight (TOF) of the recoil. By measuring the angle of the recoil and the angle and energy of the β, as well as knowing the trap position, we correct for the kinematic spread in the TOF distribution through momentum reconstruction. To the extent that we can accurately measure the β energy, we thus effectively reduce the three-body problem to two-body kinematics, and can search for additional peaks at longer TOF which would be produced by heavy neutrinos. A detailed Monte Carlo (MC) simulation is used to model the dominant decay involving a neutrino of negligible mass (ν_0) as well as one with the massive neutrino. The resulting simulations are fit to the data with the maximum likelihood (ML) method to extract the admixtures.

Our method is similar to previous measurements of the TOF of monoenergetic nuclear recoils produced in electron capture (EC) decays [6], but is free of perturbation from surfaces and is sensitive to higher neutrino mass. Previous β-recoil coincidences have been limited to extended sources and large solid-angle detectors so that no momentum reconstruction is possible [7].

The lowest neutrino mass we can resolve is 0.5 MeV. Existing experiments imply the mass of ν_μ to be less than 190 keV [8], so we are concerned here with the possible admixture in ν_e of any other heavy mass neutrino ν_x. Although there is strong evidence from atmospheric neutrinos that ν_τ has very small Δm^2 with ν_μ and ν_e, the possibility of a heavy ν_τ is not definitively excluded [2].

We trap the metastable isomer ^{38m}K ($t_{1/2} = 0.924$ s, $Q_{\beta^+} = 5.022$ MeV) produced online at TRIUMF's ISAC facility [9]. The mass-separated 30 keV ion beam is stopped in a 900 °C Zr foil and released as neutral atoms which are captured with $\approx 10^{-3}$ efficiency in a vapor-cell MOT [10]. The MOT traps only the ^{38m}K and none of the ground state ^{38}K. However, a large background arises from untrapped atoms of both ^{38}K, which decays with a 2.17 MeV γ ray, and ^{38m}K. Therefore, the trapped atoms are transferred with 75% efficiency by a laser push beam and 2D magneto-optical funnels to a second MOT equipped with the nuclear detectors, shown in Fig. 1 (see Ref. [11] for details). After transfer, the frequency and power of the second MOT beams are changed to minimize the size of the cloud. The trap lifetime, limited by residual background gas, is 45 s, so

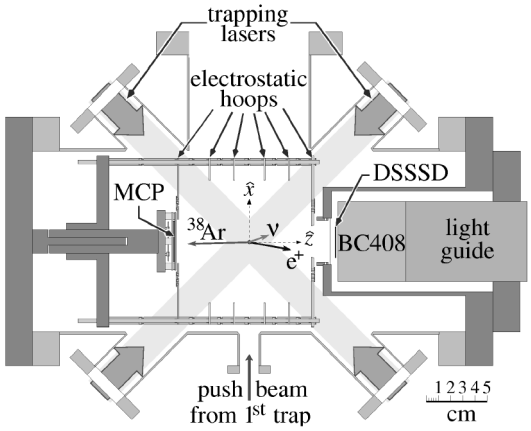

FIG. 1. Top view of the second MOT apparatus with the recoil (MCP) and β (DSSSD and BC408 scintillator) detectors.

98% of the ^{38m}K atoms decay while in the trap. The force of the MOT on the K atoms consists of near-resonant laser light and a weak (20 G/cm gradient) magnetic quadrupole field, so the Ar recoils are able to escape the trap without perturbation. Ar^- ground state ions are expected to immediately (< 1 ps) decay to the neutral Ar^0 ground state plus an electron [12]. We accelerate the positive Ar ions produced by electron shakeoff [10,13] with a uniform electrostatic field ($E_{\hat{z}} = -800$ V/cm) to separate them in TOF from the Ar^0 atoms.

The β telescope consists of a 0.49 mm thick double-sided Si-strip detector (DSSSD) with 24×24 1 mm wide strips for position sensitivity which is backed by a 6.5 cm diameter by 5.5 cm BC408 plastic scintillator with energy resolution 7.9% at 1.6 MeV. We exclude the 1 mm outer strips in X and Y from the analysis, as the collection efficiency for charge there and from Si regions outside the strip area is difficult to model and measure.

The Ar^0 recoils, which have 0–430 eV of kinetic energy, are detected by a Z stack of three microchannel plates (MCP) with 24.2 mm active diameter. Position readout is done by a resistive anode, which is absolutely calibrated with a mask and an α source. The position resolution is 0.25 mm within a 20 mm diameter; data at larger diameter have position distortions and were excluded from the analysis. The relative timing resolution between the scintillator and the MCP is 1.0 ns FWHM.

Minimizing the size of the cloud of trapped atoms, and knowing its profile and position, is very important because it is the main limitation on the timing resolution of the recoil TOF. The average $\hat{z}$ position of the trap along the detector axis is found to be 61.09 ± 0.01 mm from the MCP, determined from a fit to the leading edge of the TOF peak of the fastest Ar^0 recoils. We image the cloud by photoionizing a small fraction of the ^{38m}K atoms using a pulsed nitrogen laser. The $^{38m}K^+$ are accelerated to the MCP, and the resulting $\hat{x}$, $\hat{y}$, and $\hat{z}$ distributions can be fit very well with Gaussian peaks of 0.8, 1.1, and 0.65 mm FWHM, respectively. In addition, two CCD cameras monitor the trap position and profile in 3D by measuring the resonant fluorescence from the trap lasers. The trap centroid position was kept constant to ± 0.05 mm for the 3-week duration of the data taking.

A 2D scatter plot of the data is shown in the bottom of Fig. 2. For $m_\nu = 0$ and ideal point detectors, all the data would lie on the kinematic loci defined by the "fast" recoil branch resulting from decays in which both leptons are emitted in the same direction, or the "slow" branch with the leptons emitted in opposite directions. The corresponding loci for $m_{\nu_x} = 2$ MeV are also shown. The $\beta - \nu$ angular distribution is given by $W(\theta_{\beta\nu}) = 1 + a(v_\beta/c)\cos\theta_{\beta\nu}$, where v_β is the positron's velocity. We have chosen the pure Fermi $I^\pi = 0^+ \rightarrow 0^+$ decay of ^{38m}K, and we assume the standard model value $a = 1$. At $\theta_{\beta\nu} = 180°$, $W(\theta_{\beta\nu}) \sim 0.01$, so the vast majority of events are in the region of the fast branch and the slow branch is greatly suppressed. The branching ratio for β^+ decay to any excited state in ^{38}Ar is $< 2 \times 10^{-5}$ [14] making possible contamination negligible.

In addition to the short-lived Ar^- ground state, there is a known Ar^- metastable state with $\tau_e = 260$ ns [15] which decays by autoionization to the Ar^0 ground state [12]. If produced, these would decelerate before

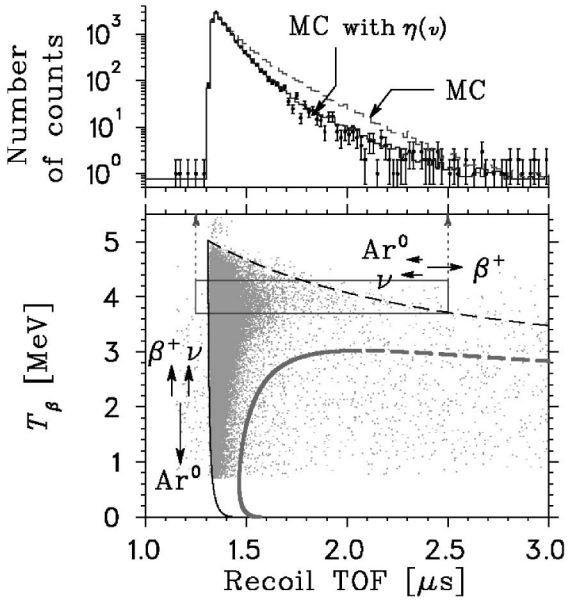

FIG. 2. Bottom: 2D scatter plot of detected β^+ energy versus recoil TOF for $\approx 60\,000$ Ar^0 events. Thin solid line: kinematic loci for "fast" branch events and pointlike back-to-back detectors. Thin dashed line: "slow" branch. The thick line shows fast and slow branches for a simulated 2 MeV neutrino. About twice as many events produce positive Ar ions, which are accelerated to TOF shorter than 1.0 μs. Ion reconstruction is kinematically more complex and is not used here. Top: Using the events contained within the box on the 2D plot, the relative MCP efficiency $\eta(v)$ is determined.

autoionizing in flight, producing events that mimic slower-TOF Ar^0. We searched for these by changing the electric field from 400 to 800 V/cm. The change in spectra at times of flight characteristic of Ar^0 was negligibly small.

The MCP efficiency for the Ar^0 detection must be modeled in the energy range of 0–430 eV. It is likely that β^+ decay of K isotopes makes neutral Ar atoms in both the atomic ground state and excited metastable (Ar^*) states, with known lifetimes of 40 and 1 s, and these would have different detection efficiencies. Using TOF data for the ν_0 slow branch in a region where ν_x would have a negligible effect (the boxed region in Fig. 2), the relative MCP efficiency as a function of v, the Ar^0 velocity, was fit to the phenomenological function

$$\eta(v) = \begin{cases} B & v < v_{\min} \\ A\left(\frac{v^2 - v_{\min}^2}{v_{\max}^2 - v_{\min}^2}\right) + B & v_{\min} \le v < v_{\max.} \end{cases}$$

B is the constant efficiency expected below a certain velocity from the Ar^* deexcitation and $A = 1 - B$ defines the relative strength of the kinetic energy-dependent contribution from electron knockout [16]. The fit, see top of Fig. 2, yielded a value of $v_{\min} = (3.5 \pm 0.8) \times 10^6$ cm/s, in accordance with other studies [17]; in our case, we found $B = 0.33 \pm 0.05$. This procedure is insensitive to the exact value of the $\beta - \nu$ correlation parameter a used, as possible nonunity values are absorbed into $\eta(v)$, and the resulting admixture error is negligible. In contrast, to determine a [10,18], the recoil ions are accelerated to an energy where the MCP efficiency is constant.

Our ability to reject events in the kinematically forbidden region is limited by three sources of background.

(1) The energy response function of the β telescope, which we model with a GEANT calculation [19], has low-energy (from bremsstrahlung, annihilation-in-flight and scattering effects) and high-energy tails (from 511 keV annihilation photons). Excluding spatially separated coincident hits in the DSSSD rejects βs that have backscattered out of the scintillator with an estimated 60% efficiency. Thus the energy-degraded events from the slow branch (Fig. 2 bottom), though modeled well, contaminate the kinematically forbidden region for ν_0.

(2) The simulation includes a small number of accidental coincidences, determined from experimental data at very long TOF. Backgrounds (1) and (2) are roughly equal at TOF=1.8 μs.

(3) The simulation has small numbers of events with incorrect kinematics from βs scattering off various volumes (MCP, chamber walls, electrostatic hoops, etc.) before entering the detector. This is checked by kinematically forbidden experimental Ar^+ ion-β coincidences.

The search for ν_x was restricted to the range $0.9 < T_\beta < 2.3$ MeV. The three-body kinematics were reduced to two-body by calculating ΔTOF, which is the difference between the directly measured TOF and that calculated from the other kinematic quantities assuming $m_\nu = 0$. For $T_\beta > 2.5$ MeV there would be two TOF solutions [20]. The reconstructed data for $1.7 < T_\beta < 1.9$ MeV are shown in Fig. 3. The width of the ΔTOF distribution is dominated by the finite trap width in $\hat{z}$.

The weak eigenstate produced by β decay in terms of the mass eigenstates and the admixture $|U_{ex}|^2$ is

$$|\nu_e\rangle = \sqrt{1 - |U_{ex}|^2}\,|\nu_0\rangle + U_{ex}|\nu_x\rangle.$$

The differential decay rate for ν_x is

$$\frac{d^3W}{dE_\beta d\Omega_\beta d\Omega_\nu} \propto p_\beta E_\beta p_\nu E_\nu \left(1 + a\frac{\vec{p}_\beta \cdot \vec{p}_\nu}{E_\beta E_\nu}\right)|U_{ex}|^2,$$

where $E_\nu = Q_{\beta^+} + m_e - E_\beta$, $p_\nu = \sqrt{E_\nu^2 - m_\nu^2}$, and the massive ν_x is only generated if $E_\nu > m_\nu$. The ν_x phase space is reduced and the angular distribution altered.

The ML method is used for a 2D search in ΔTOF as a function of β energy. The data from $T_\beta = 0.9$–2.3 MeV were divided into 0.2 MeV wide bins, and for each m_{ν_x} only kinematically allowed T_β was used. The possible ν_x was fixed in mass and its admixture $|U_{ex}|^2$ allowed to vary. Simultaneously, for each allowed T_β bin, the sum of the ν_x MC simulation and the ν_0 MC simulation was fitted to the ΔTOF spectrum of the data. The analysis was done separately for $m_{\nu_x} = 0.5$–3.6 MeV in steps of 0.1 MeV. An example of the ML fit results is shown in Fig. 3. This figure shows the comparison of the data to the fit for $m_{\nu_x} = 1$ MeV for one of the seven allowed T_β bins.

The admixture results of the full ML analysis for all masses are shown in the top of Fig. 4 and are consistent with no significant deviations from zero. The results are also interpreted as 90% confidence level upper limits

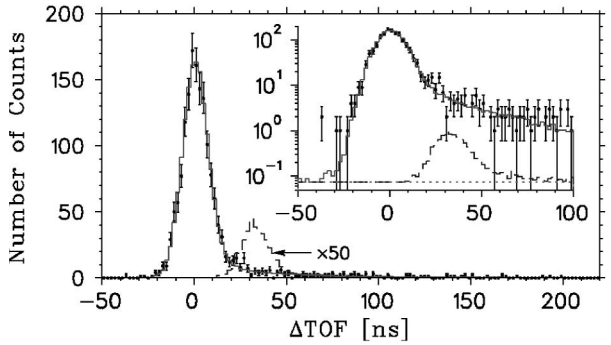

FIG. 3. The data points result from the kinematic reconstruction of events for the $T_\beta = 1.7$–1.9 MeV bin in terms of ΔTOF assuming $m_\nu = 0$ (see text). Also shown are the results of the ML fit to the data including the possible mixing of a 1 MeV ν_x. The dashed line shows the 90% confidence level upper limit of $|U_{ex}|^2 = 6 \times 10^{-3}$ for the ν_x peak as constrained by fits to all T_β bins in the log plot (inset), and ×50 for display purposes in the linear plot. The solid line shows the sum of the MC simulations (both ν_0 and ν_x) and the accidental background (dotted line).

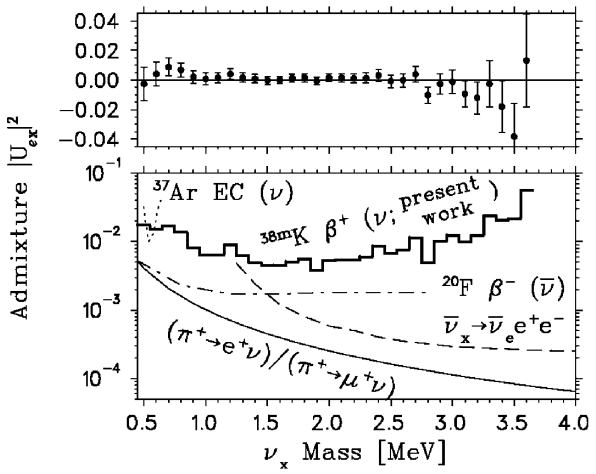

FIG. 4. Top: Deduced admixture of ν_x into ν_e. Almost the same data set is fit for each fixed m_{ν_x}, so the errors are highly correlated. Bottom: 90% confidence level upper limits on the admixture of ν_x into ν_e. Thick solid line, our limits on ν_x from ^{38m}K β^+-recoil coincidences; dotted line, ^{37}Ar EC, Ref. [6]; dash-dotted line, ^{20}F β^- shape ($\bar{\nu}_x$), Ref. [4]; dashed line, $\bar{\nu}_x \to \bar{\nu}_e e^+e^-$, Ref. [21]; thin solid line, $\pi \to e^+\nu$, Ref. [22].

which are shown in the bottom of Fig. 4, along with the results of other experiments [8]. Our results are the best model-independent direct limits on admixtures from 2.9–3.6 MeV, and are also the best direct limits on ν_e—as opposed to $\bar{\nu}_e$—admixtures with heavy ν_x for $m_{\nu_x} = 0.7$–3.6 MeV. There exist tighter limits for anti-neutrino admixtures in this mass range from a ^{20}F β^- energy spectrum measurement [4] and from a model-dependent search for $\bar{\nu}_x \to \bar{\nu}_e e^+e^-$ using reactor $\bar{\nu}_e$ [21]. A difference in heavy admixture between ν_e and $\bar{\nu}_e$ could be produced by CP violation, which is possible in the lepton sector [23]. There are better limits from the branching ratio $(\pi \to e\nu)/(\pi \to \mu\nu)$ [22], but these are indirect and subject to alteration by other new physics.

These experiments constrain a window allowed by SN1987A across this mass range, $|U_{e\,\mathrm{sterile}}|^2 \geq 0.025$ [3]. Experiments orders of magnitude better would be required to constrain sterile neutrinos as warm dark matter candidates [24], or to compete with indirect limits on heavy ν_x produced in extradimensional models [25].

Sensitivity to the ν_x ΔTOF peak scales with TOF resolution and the square root of the background. A dipole force trap could improve the cloud size and hence TOF resolution by a factor of 10. A tracking wire chamber ΔE to reject scattered β^+s and bremsstrahlung suppression for the E detector could improve the T_β response tails. Sensitivity to $|U_{ex}|^2 \sim 10^{-4}$ is foreseeable.

In summary, by using a magneto-optical trap and the new technique of full neutrino momentum reconstruction, we have set the best direct limits on heavy ν_x admixtures into ν_e (vs $\bar{\nu}_e$) for $m_{\nu_x} = 0.7$–3.6 MeV and the best model-independent direct limits from 2.9–3.6 MeV.

We acknowledge the support staff of TRIUMF and the ISAC facility, and comments by M. R. Pearson, J. N. Ng, G. C. McLaughlin, K. Abazajian, and S. H. Hansen. This work was supported by NRC through TRIUMF, by NSERC, by the Canadian Institute for Photonics Innovations, and by the Israel Science Foundation.

*Present address: MPI-K, Postfach 10 39 80, D-69029 Heidelberg, Germany.
Email address: trin@triumf.ca
†Deceased.

[1] Q. R. Ahmad *et al.*, Phys. Rev. Lett. **89**, 011301 (2002).
[2] T. Kajita and Y. Totsuka, Rev. Mod. Phys. **73**, 85 (2001).
[3] A. D. Dolgov *et al.*, Nucl. Phys. **B590**, 562 (2000).
[4] J. Deutsch, M. Lebrun, and R. Prieels, Nucl. Phys. **A518**, 149 (1990).
[5] E. L. Raab *et al.*, Phys. Rev. Lett. **59**, 2631 (1987).
[6] M. M. Hindi *et al.*, Phys. Rev. C **58**, 2512 (1998).
[7] A. Hallin *et al.*, Phys. Rev. Lett. **52**, 337 (1984).
[8] Particle Data Group, D. E. Groom *et al.*, Eur. Phys. J. C **15**, 1 (2000), and partial update for edition 2002; F. Boehm and P. Vogel, *Physics of Massive Neutrinos* (Cambridge University Press, Cambridge, 1992).
[9] M. Dombsky *et al.*, Rev. Sci. Instrum. **71**, 978 (2000).
[10] A. Gorelov *et al.*, Hyperfine Interact. **127**, 373 (2000); J. A. Behr *et al.*, Phys. Rev. Lett. **79**, 375 (1997).
[11] T. B. Swanson *et al.*, J. Opt. Soc. Am. B **15**, 2641 (1998).
[12] C. F. Bunge *et al.*, Nucl. Instrum. Methods Phys. Res. **202**, 299 (1982).
[13] T. A. Carlson *et al.*, Phys. Rev. **169**, 27 (1968).
[14] E. Hagberg *et al.*, Phys. Rev. Lett. **73**, 396 (1994).
[15] I. Ben-Itzhak *et al.*, Phys. Rev. A **38**, 4870 (1988).
[16] M. Kaminsky, *Atomic and Ionic Impact Phenomena on Metal Surfaces* (Springer-Verlag, Berlin, 1965).
[17] M. Barat *et al.*, Rev. Sci. Instrum. **71**, 2050 (2000).
[18] A. Gorelov *et al.* (to be published).
[19] CERN, GEANT version 3.12, 1994. It includes the low-energy physics of EGS4.
[20] O. Kofoed-Hansen, Dan. Mat. Fys. Med. **28**, 1 (1954).
[21] C. Hagner *et al.*, Phys. Rev. D **52**, 1343 (1995). Models with exotic ν_x decay modes soften these limits; see R. Tomàs *et al.*, Phys. Rev. D **64**, 095005 (2001).
[22] The limit shown uses the ratio from D. A. Bryman, Comments Nucl. Part. Phys. **21**, 101 (1993) and Eq. 3 of D. I. Britton *et al.*, Phys. Rev. D **46**, R885 (1992).
[23] G. Barenboim *et al.*, Phys. Lett. B **534**, 106 (2002).
[24] K. Abazajian, G. M. Fuller, and M. Patel, Phys. Rev. D **64**, 023501 (2001); A. D. Dolgov and S. H. Hansen, Astropart. Phys. **16**, 339 (2002).
[25] G. C. McLaughlin and J. N. Ng, Phys. Rev. D **63**, 053002 (2001).